Cellular/Molecular

Zcchc12-Containing Nociceptors Are Required for Noxious Heat Sensation

Dan Wu,[1]* Yan Chen,[2,3]* Zhen Li,[3] Hong Xie,[3] Sashuang Wang,[4] Yingjin Lu,[2,3,5] Lan Bao,[6,7] Xu Zhang,[1,2,3,6] and Changlin Li[2,3,5]

[1]State Key Laboratory of Neuroscience, CAS Center for Excellence in Brain Science and Intelligence Technology, Chinese Academy of Sciences, Shanghai, 200031, University of Chinese Academy of Sciences, Beijing, 100049, China, [2]Guangdong Institute of Intelligence Science and Technology, Hengqin, Zhuhai, 519031, China, [3]Research Unit of Pain Medicine, Chinese Academy of Medical Sciences; SIMR Joint Lab of Drug Innovation, Institute of Brain-Intelligence Technology, Shanghai Advanced Research Institute, Chinese Academy of Sciences (CAS); Shanghai Research Center for Brain Science and Brain-Inspired Intelligence, Shanghai, 201210, China, [4]Department of Pain Medicine and Shenzhen Municipal Key Laboratory for Pain Medicine, Huazhong University of Science and Technology Union Shenzhen Hospital, Shenzhen, 518052, China, [5]Xuhui Central Hospital, Shanghai, 200031, China, [6]School of Life Science and Technology, ShanghaiTech University, Shanghai, 201210, China, and [7]State Key Laboratory of Cell Biology, CAS Center for Excellence in Molecular Cell Science, Institute of Biochemistry and Cell Biology, Chinese Academy of Sciences, Shanghai, 200031, China

DRG neurons are classified into distinct types to mediate the somatosensation with different modalities. Recently, transcriptional profilings of DRG neurons by single-cell RNA-sequencing have provided new insights into the neuron typing and functional properties. Zinc-finger CCHC domain-containing 12 (*Zcchc12*) was reported to be the representative marker for a subtype of galanin-positive (*Gal*$^+$) DRG neurons. However, the characteristics and functions of *Zcchc12*$^+$ neurons are largely unknown. Here, we genetically labeled *Zcchc12*$^+$ neurons in *Zcchc12*-CreERT2::Ai9 mice, and verified that *Zcchc12* represented a new subpopulation of DRG neurons in both sexes. *Zcchc12*$^+$ neurons centrally innervated the superficial laminae in spinal dorsal horn, and peripherally terminated as free nerve endings in the epidermis and cluster-shaped fibers in the dermis of footpads and nearby. In addition, *Zcchc12*$^+$ neurons also formed circumferential endings surrounding the hair follicles in hairy skin. Functionally, *in vivo* calcium imaging in DRGs revealed that *Zcchc12*$^+$ neurons were polymodal nociceptors and could be activated by mechanical and noxious thermal stimuli. Behavioral tests showed that selective ablation of *Zcchc12*$^+$ DRG neurons reduced the sensitivity to noxious heat in mice. Together, we identified a new subpopulation of *Zcchc12*$^+$ nociceptors essential for noxious heat sensation.

Key words: heat nociception; mechanoheat nociceptor; *Zcchc12*

Significance Statement

Zcchc12 represents a new subpopulation of DRG neurons. The characteristics and functions of *Zcchc12*$^+$ neurons are largely unknown. Here we genetically labeled *Zcchc12*$^+$ neurons, and showed that the fibers of *Zcchc12*$^+$ DRG neurons projected to superficial lamina at spinal dorsal horn, and innervated skin as free nerve endings in the epidermis and cluster-shaped fibers in the dermis of footpads and nearby. Functionally, *Zcchc12*$^+$ DRG neurons responded to noxious mechanical and heat stimuli. Ablation of *Zcchc12*$^+$ DRG neurons impaired the sensation of noxious heat in mice. Therefore, we identify a new subpopulation of DRG neurons required for noxious heat sensation.

Introduction

Primary sensory neurons located in the DRGs are usually divided into small-size peptidergic neurons containing calcitonin-gene related peptide (CGRP), small-size nonpeptidergic neurons labeled by isolectin B4, and large-size neurons expressing neurofilament 200 (NF200) (Basbaum et al., 2009). Only the functions of CGRP-positive (CGRP$^+$) DRG neurons were explored (McCoy et al., 2013). McCoy et al. (2013) demonstrated that they could mediate the sensation of noxious heat and itch, and tonically suppress cold sensitivity. The functional diversity suggests that CGRP$^+$

DRG neurons might be divided into different subtypes with distinct functions.

The expression of functional genes in DRG neurons could indicate the properties of the neurons. For example, transient receptor potential (TRP) channels participate in thermal sensation (Dhaka et al., 2006; Julius, 2013). Piezo2, acid-sensing ion channels (ASICs), and members of potassium channel subfamily K (KCNK) are reported to be mechanotransduction channels (Noel et al., 2009; W. G. Li and Xu, 2011; Woo et al., 2015). Members of voltage-gated sodium channels (Na$_v$) contribute to noxious heat sensation (Akopian et al., 1999; Nassar et al., 2004; Yang et al., 2017). Members of MAS-related G-protein-coupled receptor (MRGPR) family play an important role in itch sensation (Han and Dong, 2014; Meixiong and Dong, 2017). Thus, the classification of DRG neurons based on the transcriptional profile of individual cell might achieve functional specificity.

Recent advances in single-cell RNA-sequencing (scRNA-seq) have provided a powerful tool to get a global view of single-cell transcriptomes at high resolution (Stuart and Satija, 2019). Several studies have classified DRG neurons by scRNA-seq (Usoskin et al., 2015; C. L. Li et al., 2016; Zheng et al., 2019; Sharma et al., 2020; K. Wang et al., 2021). Our previous study classified DRG neurons into 10 types based on the high-coverage scRNA-seq and functional annotation (C. L. Li et al., 2016). The *Sst*+ and *Mrgpra3*+ neurons were identified as distinct itching neurons (Han et al., 2013; Stantcheva et al., 2016), while the feature of *Gal*+ DRG neurons is still unclear. The *Gal*+ small-diameter could be further divided into two subtypes (C. L. Li et al., 2016). One subtype with the smallest diameter was marked by the zinc-finger CCHC domain-containing 12 (*Zcchc12*). *Zcchc12* is a transcriptional coactivator of bone morphogenic protein signaling (Cho et al., 2008), which may be involved in cancer genesis (Q. L. Li et al., 2012; O. Wang et al., 2017) and X-linked mental retardation (Cho et al., 2011). The features of *Zcchc12*-expressing DRG neurons are unknown.

In the present study, we characterized the morphologic and functional properties of *Zcchc12*+ DRG neurons. *Zcchc12*+ fibers terminated widely in hairy and glabrous skins, and innervated superficial laminae of spinal dorsal horn. *Zcchc12*+ DRG neurons functioned as polymodal nociceptors sensitive to thermal and mechanical stimulation, and were required for noxious heat sensation.

Materials and Methods

Animals

All animal studies and experimental procedures were approved by the Animal Care and Use Committee of the Institute of Neuroscience, Chinese Academy of Sciences, Shanghai, China. The *Zcchc12*-CreERT2 transgenic mouse line was generated by introducing a 2A-CreERT2 into the 3′ UTR of *Zcchc12* gene. To ablate *Zcchc12*+ DRG neurons, *Zcchc12*-CreERT2 line was crossed with *Avil*iDTR line to generate *Zcchc12*-CreERT2::*Avil*iDTR mice. *Avil*iDTR (EM: 10409) mice were purchased from the European Mutant Mouse Archive. Ai9 (JAX007909) mice were purchased from The Jackson Laboratory. All animals were housed under a 12 h light/12 h dark cycle at 22°C-26°C.

Models and surgery

In complete Freund's adjuvant (CFA) model, 20 μl CFA (Sigma, F5881) was intraplantarly injected into the left hind paw of mice of either sex. The noxious heat and mechanical threshold were measured before and 1, 2, 4, and 7 d after the injection, respectively.

In the spared nerve injury (SNI) model, mice of either sex were anesthetized by isoflurane. The skin and muscles on the left thigh were

incised to expose the sciatic nerve and its branches. The peroneal and tibial branches of the sciatic nerve were transected with ~1 mm nerve removed, leaving the sural nerve intact. The mechanical threshold was measured 2, 4, 7, and 14 d after the surgery.

Drugs

Diphtheria toxin (DTX; List Biological Laboratories, Product 150) was dissolved in 0.9% saline to make 2 mg/ml stock solution and stored at −70°C in aliquots. For *Zcchc12*+ DRG neuron ablation, tamoxifen (Sigma, T5648) was dissolved in corn oil to make 20 mg/ml solution, and was intraperitoneally injected for 5 consecutive days to induce the expression of Cre in *Zcchc12*-CreERT2::*Avil*iDTR mice of either sex at the age of 3-7 weeks. Then 200 ng/g DTX was injected intraperitoneally into the mice at the age of 10 weeks to 4 months.

ISH

Mice of either sex were anesthetized and killed; lumbar 4/5 DRGs were dissected and sectioned. For ISH, the probes were labeled with digoxigenin (DIG), while for double fluorescent ISH, the probes were labeled with DIG and FITC. DRG sections were first fixed with 4% PFA in DEPC-PBS, followed by acetylation and prehybridization in the hybridization buffer for 2.5 h at 70°C, then incubated with the hybridization buffer containing the antisense probes for 16 h at 70°C. After hybridization, the sections were washed and blocked, and sections for double FISH were pretreated with 3% H$_2$O$_2$. For ISH, sections were incubated with anti-DIG-AP antibodies (1:2000) at 4°C overnight, then were developed in a solution of 1 μl/ml NBT and 3.5 μl/ml BCIP in alkaline phosphatase buffer. For double FISH, the sections were incubated with anti-FITC-HRP (1: 4000) overnight at 4°C, then amplified with TSA-Plus (DNP, 1:100), then incubated with anti-DIG-AP (1: 1000) and anti-DNP Alexa-488 (1:500) in 1% blocking reagent overnight at 4°C. Finally, the sections were developed with HNPP/FR (1:1:100) in TS 8.0.

RNAscope ISH

DRG slides were pretreated with hydrogen peroxide at room temperature for 10 min and washed with DEPC-ddH$_2$O twice. Then, slides were slowly immersed into boiling retrieval reagent for 5 min and rinsed in the DEPC-ddH$_2$O. Then, slices were treated with ethanol for 3 min and dried completely at room temperature. Protease digestion was performed in the 40°C hybridization oven for 10-15 min and rinsed in the DEPC-ddH$_2$O twice. Then the slides were hybridized with the pre-warmed probe at 40°C for 2 h. TSA-based signal amplification was followed, and the slices were finally mounted and imaged.

In vivo *calcium imaging*

To express GCaMP6s specifically in *Zcchc12*+ DRG neurons, AAV2/9-CAG-FLEX-GCaMP6s was injected intraperitoneally into newborn *Zcchc12*-CreERT2 mice of either sex or injected into L4/5 DRGs of adult *Zcchc12*-CreERT2 mice of either sex.

The lumbar 4/5 DRG was exposed by surgery. Various stimuli were applied to the hind paw of mice. The intensity of calcium fluorescence was recorded in real time by a Leica Microsystems SP8 DIVE multiphoton microscope and Prairie (Ultima-IV) two-photon microscope. The laser was set to 920 nm for GCaMP6s imaging. For thermal stimulation, we used hot water at 50°C-60°C. For mechanical stimulation, we chose nocuous pinch and pressure, and innocuous brush and air puff. There were 3-5 min intervals between any two thermal or mechanical stimuli to avoid sensitization.

Whole-mount immunohistochemistry

Before hair skin dissection, the mice of either sex were treated with hair remover, wiped clean with tissue paper, and tape stripped until glistening. Glabrous skin of hind paw and hairy skin of back were dissected after mice were anesthetized. The skin was then flattened and fixed in Zamboni's buffer overnight at 4°C. The tissues were washed with PBS containing Triton X-100 (0.3% PBST every 30 min for hairy skin and 1% PBST every hour for glabrous skin) for 5-8 h, and then incubated with primary antibodies in PBST containing 5% donkey serum and 20% DMSO for 5 d at room temperature. After the conjunction of primary antibodies, tissues were washed with PBST for 5-8 h, and then incubated

with secondary antibodies (dilution buffer the same with primary antibodies) for 2 d at room temperature. Tissues were washed with PBST and dehydrated with methanol. Hairy skin was dehydrated in 50% methanol for 5 min and then in 100% methanol for 20 min, 3 times, while glabrous skin was dehydrated in methanol overnight. Finally, the tissues were cleared and stored in BABB (benzyl alcohol, Sigma 402834; benzyl benzoate, Sigma B-6630; 1:2). The tissues were imaged by Leica Microsystems SP8 confocal microscope and processed in ImageJ software.

Immunohistochemistry
Mouse glabrous and hairy skin was dissected and fixed as mentioned above. The skin was dehydrated in 30% sucrose solution at 4°C, then sectioned into 50 μm by Leica Microsystems CM 1950, and floated in PBS. For skin section staining, the floating slices were blocked in PBS containing 0.5% Triton X-100 and 5% BSA for 1 h at room temperature. Then the sections were incubated with primary antibodies in PBS containing 3% BSA overnight at 4°C. The sections were then washed with PBS and incubated with secondary antibodies for 1 h at room temperature. Finally, the sections were washed with PBS and mounted on glass slides.

For the DRG staining, mice were fixed with 4% PFA, and the DRGs were dissected and sectioned. After blocked with PBS containing 0.05% Triton X-100 and 10% donkey serum, sectioned slices were incubated with primary antibodies overnight at 4°C, followed with secondary antibodies for 40 min at room temperature, and finally mounted. The slides were imaged by Leica Microsystems SP8 confocal microscope.

Behavior tests
All behavior tests were conducted blindly. Mice of either sex were habituated in the experimental environment for over 3 d before formal behavioral tests.

Hargreaves test. Mice were habituated in plastic chambers, the radiant light was applied to the left hind paw of mice when they were resting quietly, and the latency to paw withdraw was measured. The cutoff time was set at 20 s.

Hot plate test. Mice were put on a hot plate at a temperature of 52°C. The latency to jump, shake, or lick the hind paw was measured. The cutoff time was set at 30 s.

Tail immersion test. One-third of mouse tail was immersed in water bath at 52°C, and the latency to flick the tail was measured. The cutoff time was set at 10 s.

von Frey test. Mice were habituated in small plastic chambers on a mesh floor, and the mechanical threshold was assessed by measuring the 50% paw withdrawal with a series of von Frey filaments or the frequency of withdrawal.

Acetone test. Mice were placed on a mesh floor, 50 μl of acetone was add to the left hind paw, and the number of lickings was measured for 1 min.

Icilin test. Icilin (60 μg in 25 μl volume) was injected into the left hind paw of mice, and the number of flinches in 10 min was counted. Icilin is dissolved in 10% DMSO, 40% PEG400, 5% Tween-80, and 45% saline.

Cotton swab assay. The left plantar surface of mice was stroked with fluffy cotton swab for 20 times with intervals over 10 s. The number of paw withdrawals was recorded.

Experimental design and statistical analysis
Analyses were performed with the person analyzing the data blind to experimental condition. Data are presented as mean ± SEM. Sample number (n) values are indicated in the figure legends and in Results. For morphologic analyses, sections of 3 mice (three sections/mouse) were used. Two groups were compared by a two-tailed, unpaired Student's t test. Comparisons between two groups with multiple times were performed by a two-way ANOVA with Bonferroni's correction. Statistical analysis was performed using PRISM (GraphPad Software). The difference was considered significant at $p < 0.05$. All statistical analyses were two-tailed, 95% CI.

Results

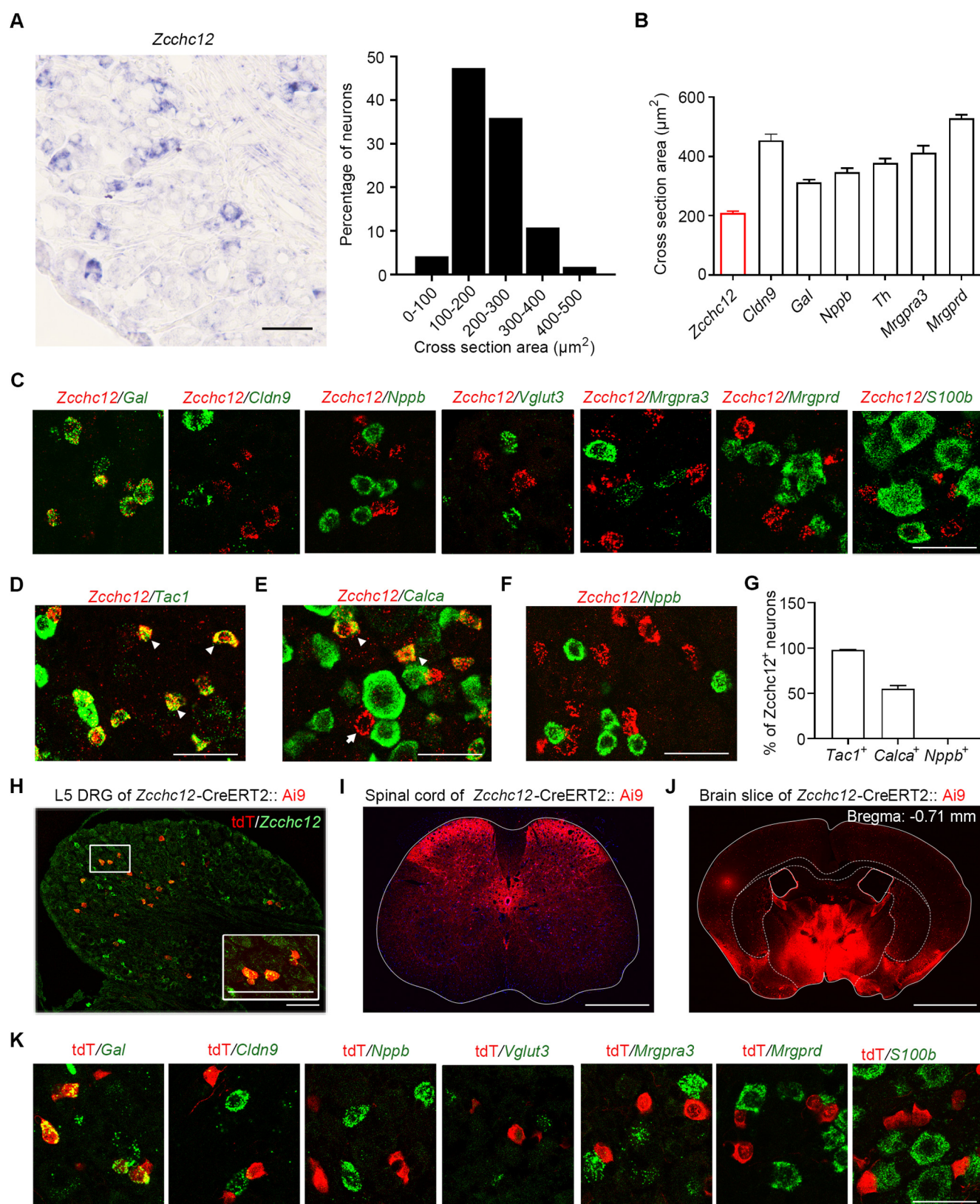## *Zcchc12* represents a subpopulation of *Gal*[+] peptidergic DRG neurons

Classification of DRG neurons based on single-cell transcriptomes has revealed that *Zcchc12*^{+} and *Cldn9*^{+} DRG neurons were two subtypes of *Gal*[+] neuron type (C. L. Li et al., 2016). *Zcchc12* was expressed in 12.60 ± 0.77% of DRG neurons. The majority of them were small-diameter neurons (cross-section area < 800 μm^2) (Fig. 1A). We compared the average size of *Zcchc12*^{+} DRG neurons with other types of small-diameter DRG neurons. The average cross-section areas of *Zcchc12*^{+}, *Cldn9*^{+}, *Gal*[+], *Nppb*[+], *Th*[+], *Mrgpra3*^{+}, and *Mrgprd*^{+} DRG neurons were 209.8 ± 5.8, 453.7 ± 21.94, 313.4 ± 8.12, 346.6 ± 14.0, 378.4 ± 14.1, 412.2 ± 24.2, and 529.2 ± 11.1 μm^2, respectively (Fig. 1B). Thus, *Zcchc12*^{+} neurons are the smallest DRG neurons.

In WT mice, most of *Zcchc12*^{+} neurons (87.8 ± 1.4%) were *Gal*[+] and *Cldn9*^{−}, and 55.7 ± 3.1% of *Gal*^{+} neurons coexpressed *Zcchc12* (Fig. 1C). To validate the expression specificity of *Zcchc12*, we examined the coexpression of *Zcchc12* with the marker genes of other types of small-diameter DRG neurons (Fig. 1C). Most of Zcchc12^{+} DRG neurons (98.1 ± 0.5%) were *Tac1*^{+}, but only 39.9 ± 2.0% of *Tac1*^{+} neurons coexpressed *Zcchc12* (Fig. 1D,G). In addition, only about half of the *Zcchc12*^{+} DRG neurons (54.9 ± 3.8%) were *Calca*[+] (Fig. 1E,G), and none of them was *Nppb*[+] (Fig. 1F). This evidence showed that Zcchc12 represents a new subtype of peptidergic neurons.

Zcchc12-CreERT2 transgenic mice were constructed and bred with the *Ai9* mice to visualize *Zcchc12*^{+} neurons. The expression of tdTomato could be detected in the DRG, spinal cord, and brain (Fig. 1H–J). In the lumbar DRG, ~69% *Zcchc12*^{+} DRG neurons were labeled by tdTomato (Fig. 1H). The distribution of the tdTomato^{+} neurons was similar with that of *Zcchc12*^{+} neurons. The types of DRG neurons and the percentage of each type in the transgenic mice were in accordance with those in WT mice. *Zcchc12* mRNA was detected in 78.66 ± 3.3% of tdTomato-labeled neurons (Fig. 1H). To evaluate the ectopic Cre recombination, we examined the expression of tdTomato in other types of DRG neurons. Double fluorescent ISH showed that tdTomato was mainly expressed in *Gal*[+] and *Cldn9*^{−} neurons (Fig. 1K) but rarely expressed in the *Il31ra*^{+}, *Th*[+], *Mrgpra3*^{+}, or *Mrgprd*^{+} neurons (Fig. 1K). As expected, *Zcchc12*-CreERT2::Ai9 mouse line could be used to examine the feature of *Zcchc12*^{+} neurons. Together, *Zcchc12* in the DRG genetically represents a subpopulation of *Gal*^{+} neurons, which are the smallest somatosensory neurons.

Zcchc12^{+} DRG neurons project to the superficial laminae of spinal cord

The spinal cord is organized into anatomic and electrophysiological laminae (Kandel et al., 2013). Different laminae receive information from distinct types of DRG neurons mediating different types of stimuli (Meyer et al., 2006; Basbaum et al., 2009; Abraira and Ginty, 2013). Given that *Zcchc12* is expressed not only in the DRG but also in the spinal cord, we specifically labeled *Zcchc12*^{+} DRG neurons in *Zcchc12*-CreERT2 transgenic mice by either DRG micro-injection or intraperitoneal injection with a Cre-depended adeno-associated virus (AAV2/9-CAG-DIO-mCherry) (Fig. 2A). *Zcchc12*^{+} DRG neurons infected by AAV could be labeled by the fluorescent protein mCherry after tamoxifen induction (Fig. 2B). *Zcchc12*^{+} fibers mainly innervated laminae I and II $_{outer}$ of spinal cord, and most of them were colocalized with CGRP (Fig. 2C). Some CGRP-negative

Figure 1. *Zcchc12* genetically represented a subpopulation of *Gal*^{+} DRG neurons. ***A***, ISH showed the expression of *Zcchc12* in a lumbar DRG. Histogram represents the size distribution of *Zcchc12*^{+} DRG neurons. Scale bar, 50 μm. ***B***, Histogram represents the size distribution of *Zcchc12*^{+}, *Cldn9*^{+}, *Gal*[+], *Nppb*[+], *Th*[+], *Mrgpra3*^{+}, and *Mrgprd*^{+} DRG neurons. ***C***, RNAscope ISH showed the localization of the *Zcchc12* with *Gal*, *Cldn9*, *Nppb*, *Vglut3*, *Mrgpra3*, *Mrgprd*, and *S100b* in the lumbar DRG of the WT C57 mouse. Scale bar, 50 μm. ***D-F***, RNAscope ISH showed coexpression of *Zcchc12* with *Tac1*, *Calca*, and *Nppb*. Scale bar, 50 μm. ***G***, Histogram represents the percentage of the colocalization with *Zcchc12*^{+} neurons. ***H-J***, Expression of tdTomato in the lumbar DRG, spinal cord, and brain of the *Zcchc12*-CreERT2::Ai9 transgenic mouse. Scale bar, 100 μm. ***K***, RNAscope ISH showed the expression of tdTomato and *Gal*, *Cldn9*, *Nppb*, *Vglut3*, *Mrgpra3*, *Mrgprd*, and *S100b* in the lumbar DRG of *Zcchc12*-CreERT2::Ai9 transgenic mice. Scale bar, 50 μm.

A

Zcchc12-CreER

B

Zcchc12-CreER AAV-DIO-mCherry

C

Lumbar spinal cord

D

Lumbar spinal cord
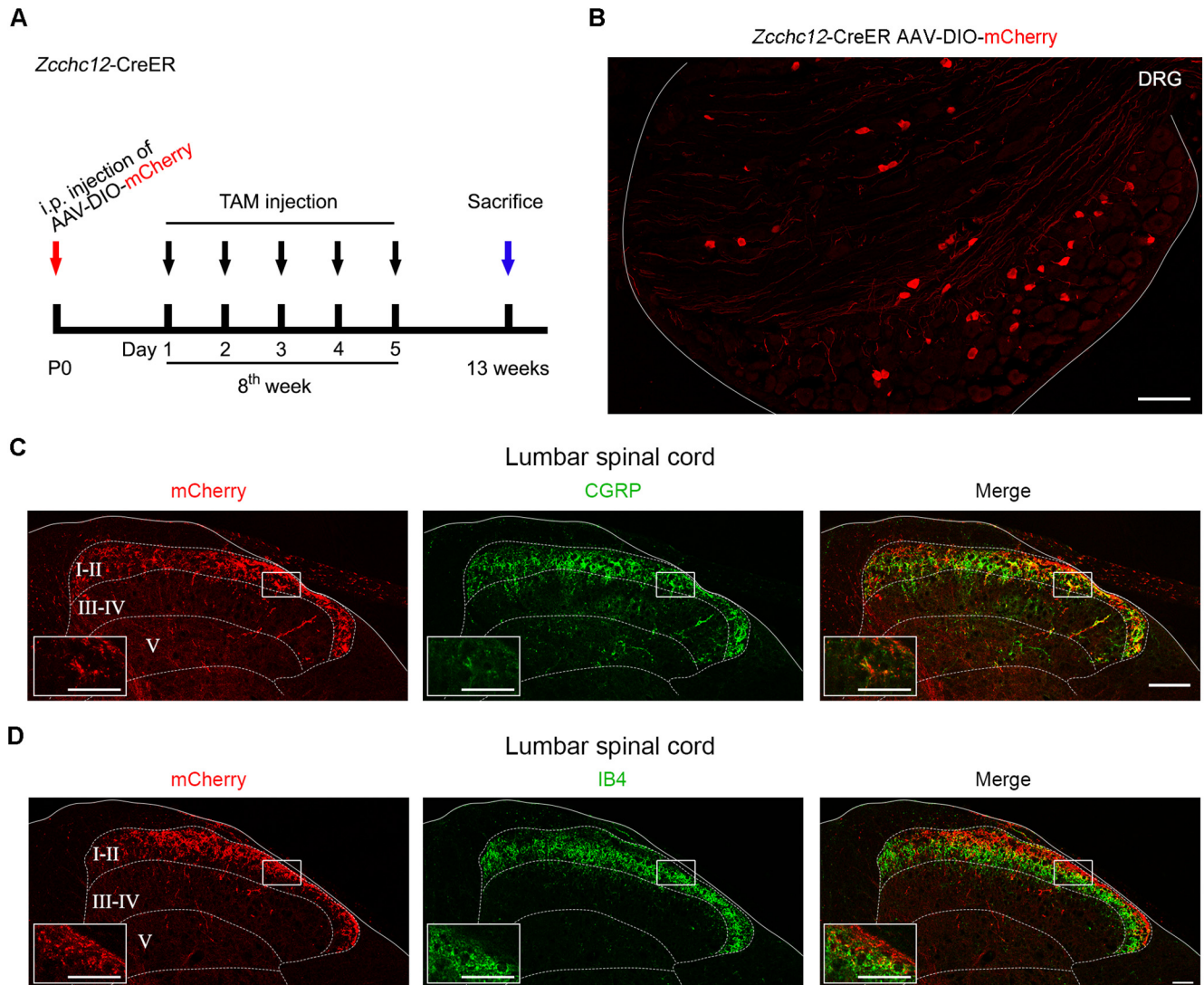
Figure 2. Zcchc12$^+$ terminals centrally projected to the superficial laminae of the spinal dorsal horn. **A**, Schematic paradigm showing infection strategy of DRG neurons by AAV intraperitoneal injection. **B**, Zcchc12$^+$ DRG neurons were labeled by AAV injected intraperitoneally. Scale bar, 100 μm. **C**, Colocalization of mCherry and CGRP in the spinal cord. Scale bar, 100 μm. **D**, Colocalization of mCherry and IB4 in spinal cord. Scale bar, 100 μm. i.p., Intraperitoneal; TAM, tamoxifen.
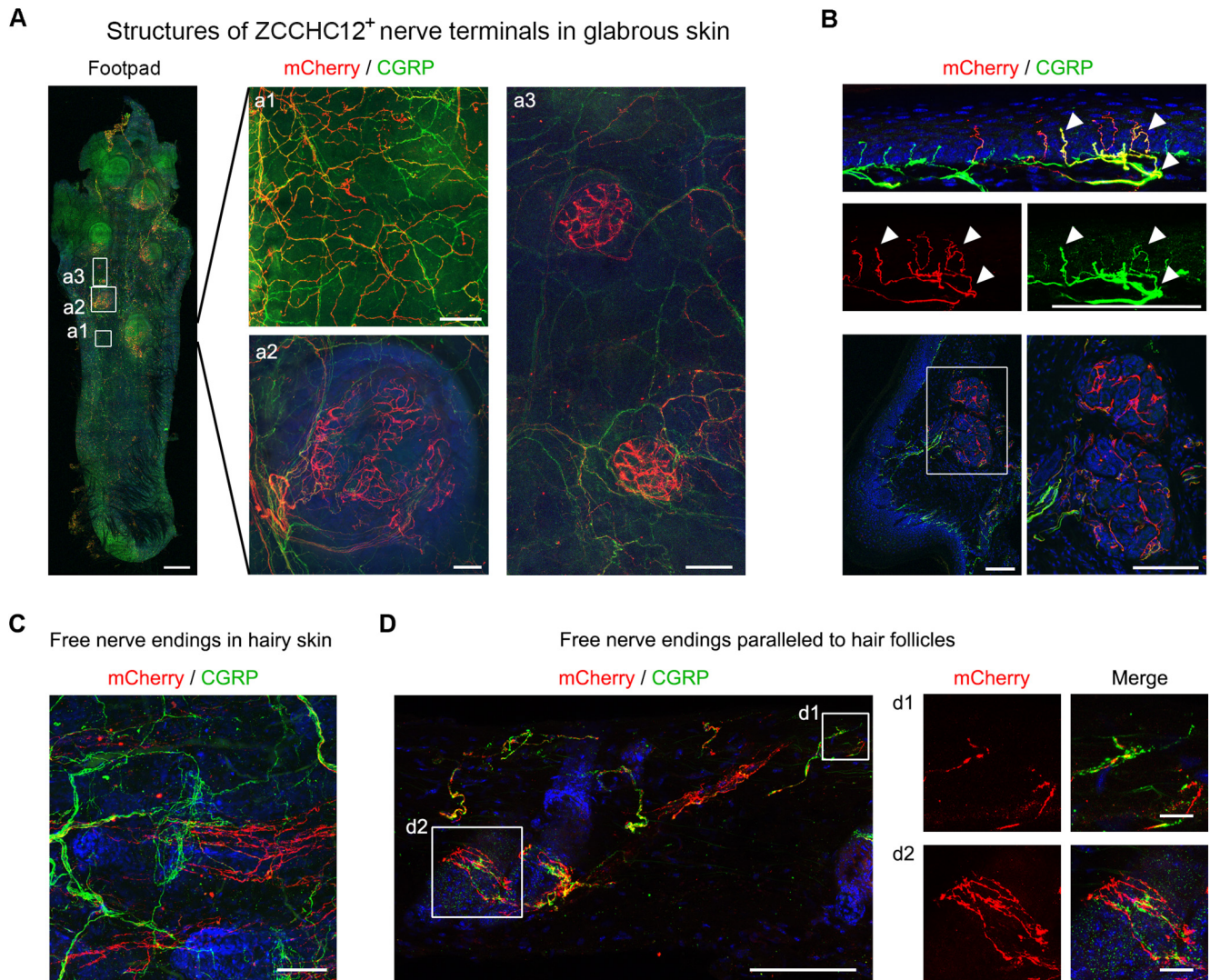
Zcchc12$^+$ fibers have also been observed in the most superficial lamina, indicating that there were two types of Zcchc12$^+$ fibers. Zcchc12$^+$ fibers rarely terminated in spinal lamina II$_{inner}$, which was labeled by the IB4 (Fig. 2D). Together, this projection pattern indicated that Zcchc12$^+$ DRG neurons could function as peptidergic nociceptors.

Zcchc12$^+$ DRG neurons innervate the skin with diverse terminals

Using the viral strategy, we examined the cutaneous terminals of Zcchc12$^+$ DRG neurons in the skin of Zcchc12-CreERT2 transgenic mice (Fig. 3). Immunostaining of whole-mount skins or tissue sections was performed to determine the distribution of Zcchc12$^+$ nerve terminals in the skin (Fig. 3A,B). Peptidergic CGRP$^+$ neurons innervate skin (McCoy et al., 2012). Since most of the Zcchc12 was colocalized with CGRP in central terminals, we also determined the peripheral targets of Zcchc12$^+$ neurons using CGRP as a positive control. In the glabrous skin, Zcchc12$^+$ free nerve endings were observed in the epidermis (Fig. 3Aa1,B). Most of the labeled free nerve endings were

coexpressed with the CGRP in free nerve endings (Fig. 3B). This observation supported the hypothesis that Zcchc12$^+$ DRG neurons could function as peptidergic nociceptors. In addition, specialized Zcchc12$^+$ terminals shaping like a dense cluster could be observed in the glabrous skin. The clustered dense terminals were observed within and surrounding the derma of the footpad (Fig. 3Aa2,a3,B). The specialized cluster has never been termed or functionally studied before. Furthermore, CGRP did not colocalize with Zcchc12 in the specialized cluster (Fig. 3B).

Zcchc12$^+$ DRG neurons also innervated the hairy skin. Whole-mount immunohistochemistry for mCherry showed that Zcchc12$^+$ free nerve endings were in hairy skin (Fig. 3C). The direction of the free nerve endings was paralleled to the hair follicles (Fig. 3Dd1). Thus, in addition to the glabrous skin, Zcchc12$^+$ DRG neurons might also mediate noxious stimulation of the hairy skin. We also observed Calca$^-$/Zcchc12$^+$ circumferential endings surrounding hair follicles (Fig. 3Dd2). Two types of circumferential endings have been reported before. One is Nefh$^+$ myelinated low-threshold mechanoreceptors (L. Li et al., 2011; Bai et al., 2015), and the other is Calca$^+$ high-threshold

A Structures of ZCCHC12+ nerve terminals in glabrous skin

B

C Free nerve endings in hairy skin

D Free nerve endings paralleled to hair follicles

Figure 3. *Zcchc12*+ DRG neurons peripherally innervated various cutaneous receptors in skin. **A**, Whole-mount immunostaining of the hind paw of a mouse showed the morphology of ZCCHC12+ terminals in glabrous skin. Scale bar, 1 mm. Enlarged images showed the free nerve endings (**a1**), the clustered dense terminals in the footpad (**a2**), and the specialized terminals surround footpad (**a3**). Scale bars: **a1-a3**, 100 μm. **B**, Representative image of sections of the glabrous skin showed the ZCCHC12+ free nerve endings in the glabrous skin (top) and the clustered dense terminals in the footpad (bottom). Scale bar, 100 μm. **C**, Whole-mount immunostaining showed the ZCCHC12+ terminals in the hairy skin. Scale bar, 50 μm. **D**, Representative image of sections showed the *Zcchc12*+ terminals in the hairy skin. Enlarged images showed the circumferential endings (**d1**) and free nerve endings (**d2**) in hairy skin. Scale bars: **d1**, 20 μm; **d2**, 10 μm.

mechanoreceptors (Ghitani et al., 2017). The ZCCHC12+ circumferential endings were neither of them, which suggested a new type of ZCCHC12+ circumferential endings.

Together, *Zcchc12*+ DRG neurons innervate glabrous and hairy skin with various structures, including free nerve ending, specialized nerve cluster, and circumferential endings. These results indicate that *Zcchc12*+ DRG neurons could mediate the sensations of different modalities in both glabrous and hairy skin.

Zcchc12+ DRG neurons respond to noxious thermal and mechanical stimuli

To explore the functions of *Zcchc12*+ DRG neurons, we adopted *in vivo* two-photon calcium imaging to evaluate the physiological features of *Zcchc12*+ DRG neurons. We injected AAV2/9-CAG-FLEX-GCaMP6s, a Cre-dependent recombinant AAV encoding the calcium sensor GCaMP6s, into L4 or L5 DRG of *Zcchc12*-CreERT2 mice. After inducing the expression of GCaMP6s, we conducted *in vivo* two-photon calcium imaging on DRG to determine the responses of GCaMP6s-expressing neurons to

noxious heat, cold, mechanical stimuli, as well as innocuous puff and brush. We delivered the stimulation on the hind paw of mice. The real-time calcium signals were recorded and analyzed.

In total, 130 responsive neurons were analyzed. In general, Ca^{2+} signals in *Zcchc12*+ DRG neurons were induced by noxious heat, cold, and mechanical stimuli but not by innocuous puff and brush (Fig. 4A–C). Of the 130 responsive neurons, ~68% of the responsive neurons responded to noxious heat (52°C), 54% to noxious mechanical stimuli (pressure or pinch), and 16% to noxious cold (0°C) (Fig. 4D). Thus, *Zcchc12*+ DRG neurons were nociceptors that could detect noxious thermal or mechanical stimuli. A large proportion of neurons (84 of 130) responded to only one type of stimulation. Among them, 59 neurons were sensitive to thermal stimuli and 25 to mechanical stimuli (Fig. 4C,E,F). Other neurons (46 of 130 neurons) responded to at least two types of stimulation (Fig. 4C,E,F). However, only a few (4 of 130) responded to heat, cold, and mechanical stimuli (Fig. 4D–F). Among these responsive neurons, >60% of either mechanical-sensitive or cold-sensitive neurons were polymodal, whereas ~40% of heat-sensitive
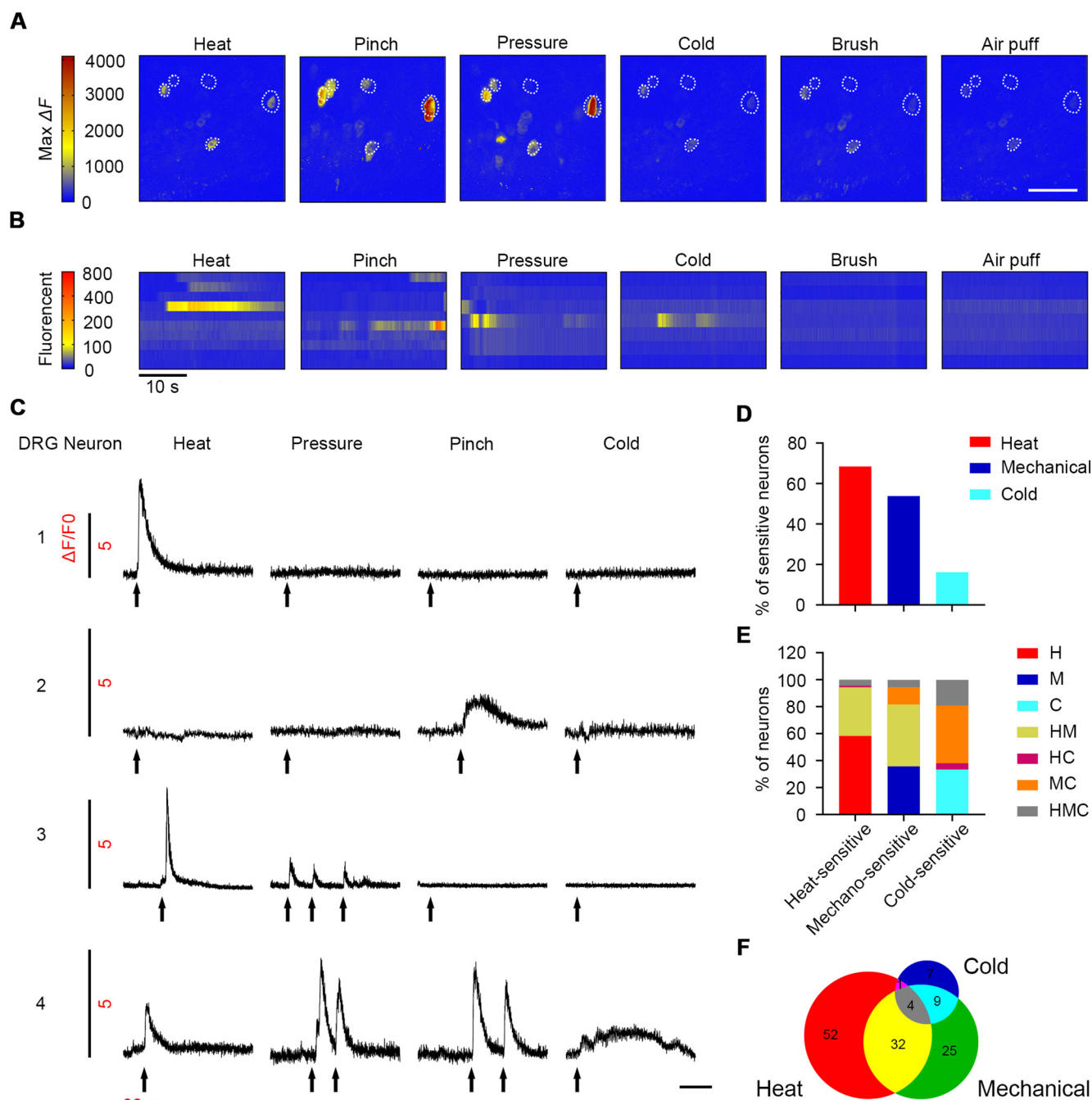
Figure 4. Zcchc12⁺ DRG neurons were nociceptors responding to noxious thermal and mechanical stimuli. ***A***, Heatmap of a typical imaging field showing Ca²⁺ signals of neuron responses to noxious heat, cold, noxious mechanical, and innocuous mechanical stimuli. Color scale represents the maximum ΔF. Scale bar, 100 μm. ***B***, Heatmap of Ca²⁺ signals of neurons from a single imaging field to a series of stimuli. Color scale represents the ΔF/F0. Calibration: 10 s. ***C***, Representative Ca²⁺ curves indicate typical responses of 4 neurons to thermal and mechanical stimuli. Different ΔF/F0 scales for different neurons. Arrows indicate beginning of stimuli. ***D***, Proportion of neurons activated by each type of stimulus. ***E***, Proportions of neurons with distinct responsive modality in heat-, mechano-, and cold-sensitive neurons. ***F***, Diagrams represent overlap in neurons responsive to heat, mechanical, and cold stimuli.

Zcchc12⁺ neurons were polymodal. Therefore, these results indicate that Zcchc12⁺ DRG neurons are polymodal nociceptors and could be divided functionally. A small portion of Zcchc12⁺ DRG neurons could participate in cold sensation.

Ablation of Zcchc12⁺ DRG neurons causes the defect in heat sensitivity

To explore the functions of Zcchc12⁺ DRG neurons, we selectively ablated Zcchc12⁺ neurons in the peripheral nervous system. We adopted a transgenic mouse with a Cre-dependent DTX

receptor (DTR) driven from the *Avil* locus (Stantcheva et al., 2016), and generated Zcchc12-CreERT2:Avil^iDTR mice. After the induction of DTR, the application of DTX could lead to selective deletion of Zcchc12⁺ neurons in sensory ganglia. First, we found that the homozygous (Cre⁺/⁺), heterozygous (Cre⁺/⁻), and hemizygous (Cre⁺/Y) of transgenic mice showed similar nociceptive threshold to their littermate control mice in responding to thermal and mechanical stimuli (Fig. 5A–D). DTX treatment did not cause heat hypoalgesia in genetic control animals (Fig. 5E,F). Then, we ablated Zcchc12⁺ DRG neurons by injecting
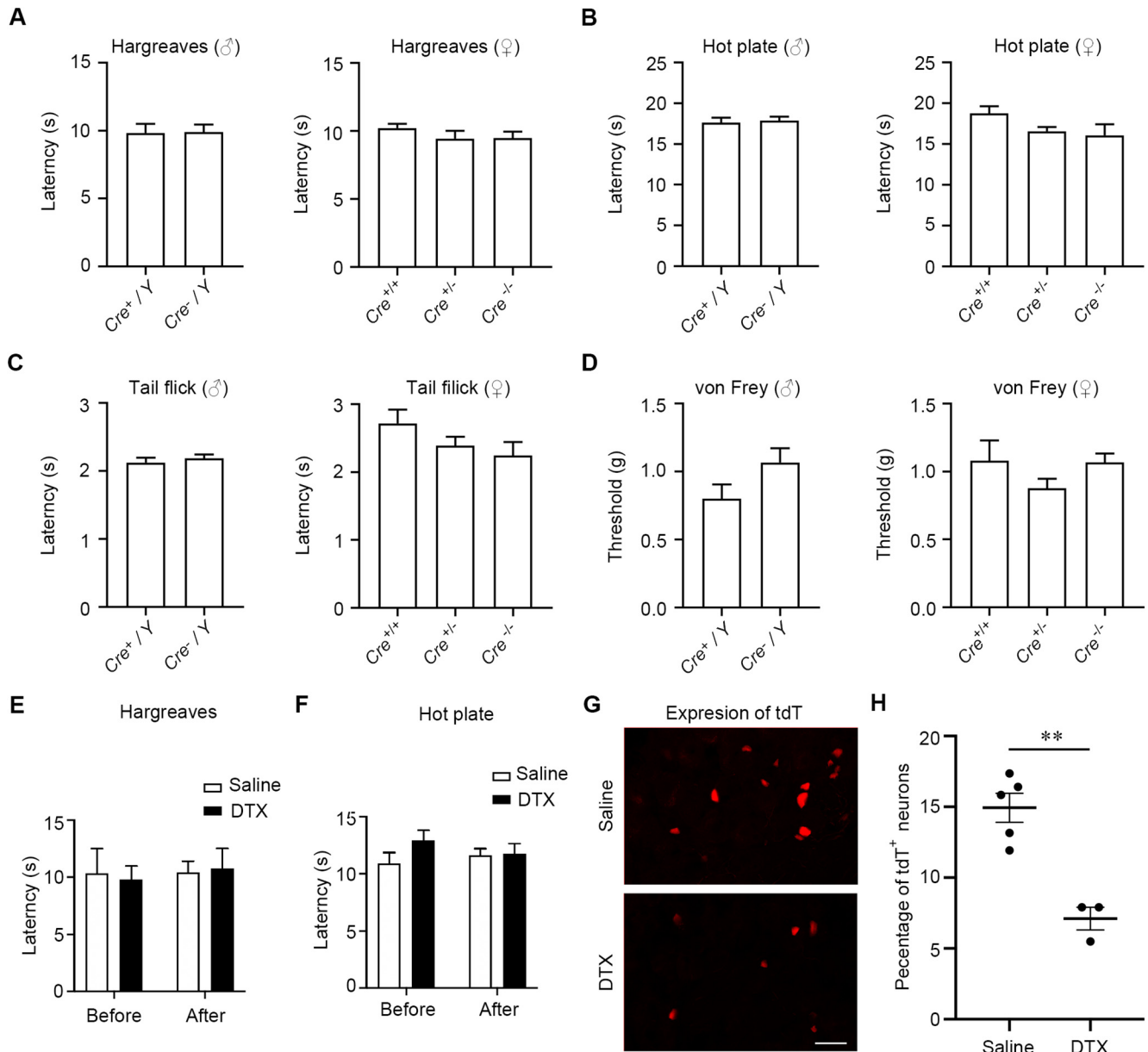
Figure 5. The transgenic mice have normal thermal and mechanical perception. ***A-C***, Hargreaves, hot plate, and tail flick results showed no significant difference in the noxious heat response among the *Cre*⁺ and *Cre*⁻ mice. *n* ≥ 5 for each group. ***D***, von Frey showed the mechanical sensitivity unchanged in the *Cre*⁺ and *Cre*⁻ mice. *n* ≥ 5 for each group. ***E, F***, Histogram showed that DTX injection did not affect the noxious heat sensation in WT mice. ***G, H***, The percentage of tdTomato⁺ (tdT⁺) neurons was significantly decreased in the *Zcchc12*-CreERT2::*Avil*ⁱᴰᵀᴿ::Ai9 mice after DTX treatment. Scale bar, 50 μm. **$p = 0.0019$.

DTX in *Zcchc12*-CreERT2:*Avil*ⁱᴰᵀᴿ mice. DTX administration ablated about half of the tdTomato-labeled neurons in L5 DRG compared with that treated by saline (Fig. 5*G,H*). We performed behavioral tests before and after the injection to evaluate the effect of genetic ablation on pain behavior. The sensation of noxious heat was examined by the Hargreaves and hot plate tests. Before the toxin administration, mice presented comparable withdraw latency in both tests. The ablation of *Zcchc12*⁺ DRG neurons significantly increased the latency of withdrawal of the hind paw receiving noxious heat stimulation (Fig. 6*A, B*). There was no significant change in withdrawal behavior induced by icilin or acetone administration after the ablation of *Zcchc12*⁺ DRG neurons (Fig. 6*C,D*). For mechanical nociception, the selective ablation had no significant effect on withdrawal threshold (Fig. 6*E*) or withdrawal percentage

at von Frey test (Fig. 6*F*). The cotton swab and tape response assay were used to test the sensitivity to innocuous mechanical stimulation (Garrison et al., 2012). No significant difference could be found in the innocuous mechanical test after toxin administration (Fig. 6*G,H*). Therefore, the results indicate that *Zcchc12*⁺ DRG neurons play important roles in thermal nociception under physiological condition.

Then we asked whether *Zcchc12*⁺ DRG neurons contributed to pain sensitization under pathologic conditions. In the CFA inflammatory model that causes mechanical and heat hypersensitivity, the toxin- and saline-treated mice showed equivalent heat and mechanical hypersensitivity (Fig. 6*I–K*). In the SNI model of neuropathic pain, the ablation of *Zcchc12*⁺ DRG neurons did not alter the mechanical allodynia in the toxin-treated mice (Fig. 6*L*). In conclusion, *Zcchc12*⁺ DRG neurons played
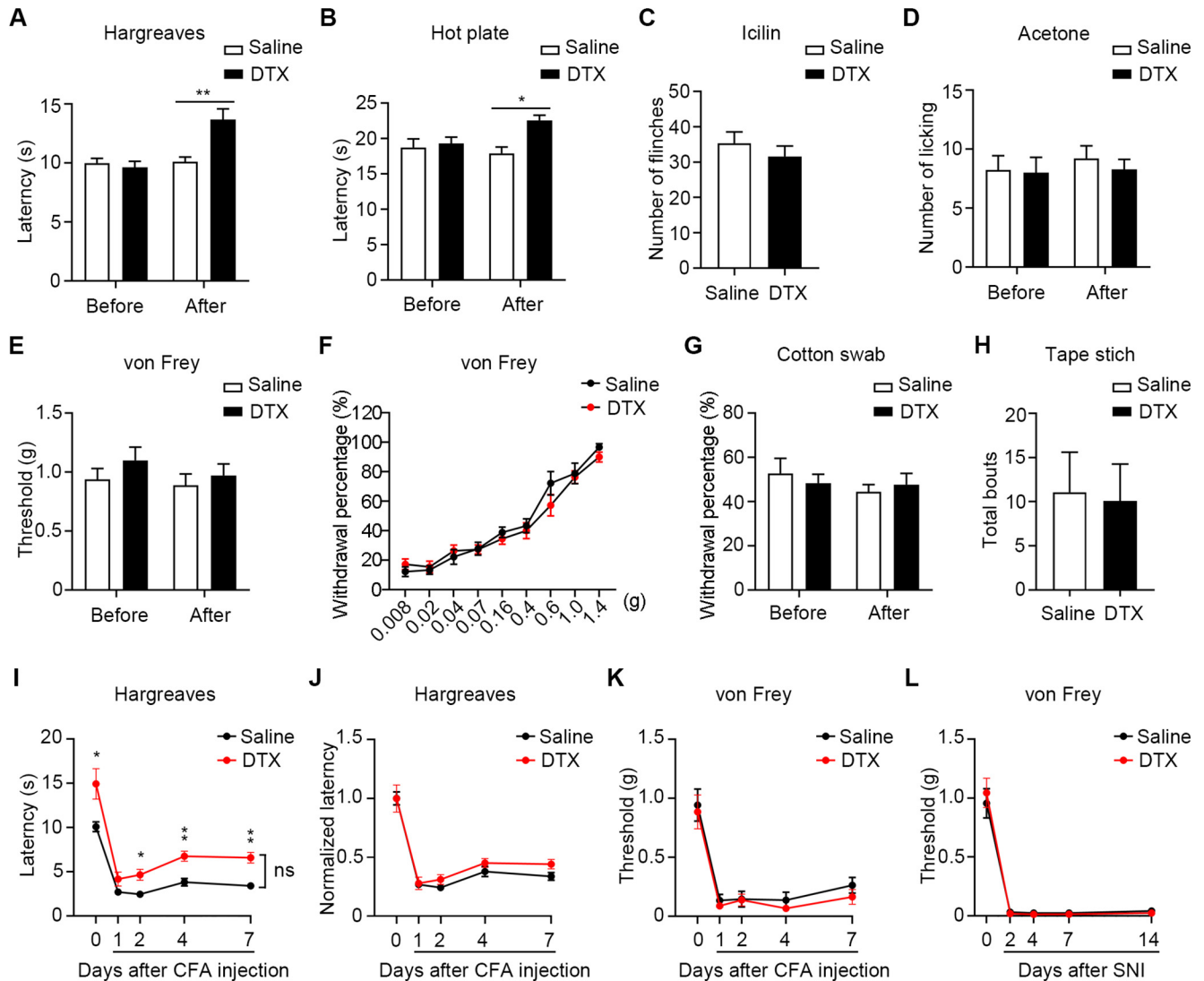
Figure 6. *Zcchc12*^{+} DRG neurons were necessary for noxious heat sensation. ***A***, Hargreaves results showed significant increase of the response latency for noxious heat in mice with *Zcchc12*^{+} DRG neurons ablated. Cutoff, 20 s. *n* = 16 for DTX-treated mice and *n* = 16 for saline-treated mice. **p = 0.0016. ***B***, Hot plate (52℃) results showed that the latency for noxious heat was significantly increased in DTX-treated mice compared with the saline-treated mice. Cutoff, 30 s. *n* = 7 for both DTX- and saline-treated mice. *p = 0.0025. ***C***, Icilin test showed that sensitivity to cold was unchanged after ablation of *Zcchc12*^{+} DRG neurons. *n* = 10 for DTX-treated mice and *n* = 9 for saline-treated mice. ***D***, Acetone test showed that sensitivity to cold was unchanged after ablation of *Zcchc12*^{+} DRG neurons. *n* = 12 for DTX-treated mice and *n* = 9 for saline-treated mice. ***E***, von Frey results showed that there was no significant difference between the mechanical threshold between DTX-treated mice and saline-treated mice. *n* = 14 for DTX-treated mice and *n* = 16 for saline-treated mice. ***F***, von Frey showed the mechanical sensitivity unchanged in DTX-treated mice. *n* = 12 for DTX-treated mice and *n* = 9 for saline-treated mice. ***G***, ***H***, Cotton swab test and tape stich test showed the sensitivity to light touch unchanged after DTX treatment. In cotton swab test, *n* = 12 for DTX-treated mice and *n* = 9 for saline-treated mice. In tape stich test, *n* = 11 for DTX-treated mice and *n* = 9 for saline-treated mice. ***I***, Hargreaves results showed the heat hyperalgesia in saline- and DTX-treated mice after CFA injection. *n* = 7 for both DTX- and saline-treated mice. *p = 0.0305, *p = 0.0117, **p = 0.0018, and **p = 0.0012 for 0, 2, 4, and 7 d after CFA injection, respectively. ***J***, Normalized noxious heat threshold showed that the heat hyperalgesia in DTX-treated mice was similar with control group after CFA injection. *n* = 7 for both DTX- and saline-treated mice. ***K***, von Frey results showed that the mechanical hyperalgesia in DTX-treated mice was similar with control group after CFA injection. *n* = 7 for both DTX- and saline-treated mice. ***L***, von Frey results showed that the mechanical hyperalgesia in DTX-treated mice was similar with control group after SNI. *n* = 9 for both DTX- and saline-treated mice. Data are mean ± SEM. ***A–E***, ***G***, ***H***, Two-tailed unpaired *t* test. ***F***, ***I–L***, Two-way ANOVA test followed by Bonferroni correction.

roles mainly in physiological heat nociception but not in the initiation or maintenance of pathologic pain.

Discussion

The present study demonstrates the peripheral and central innervations, and the functions of *Zcchc12*^{+} DRG neuron. In spinal dorsal horn, the fibers of *Zcchc12*^{+} DRG neurons innervate superficial laminae. In skin, *Zcchc12*^{+} fibers terminate in multiple shapes. Functionally, *Zcchc12*^{+} DRG neurons are polymodal nociceptors. Behaviorally, they are required for the sensation of noxious heat, but not noxious mechanical and cold stimuli.

These findings reveal that the *Zcchc12*^{+} DRG neuron, a new subpopulation of nociceptors, is required for noxious heat sensation.

***Zcchc12*^{+} DRG neuron is a new subpopulation of nociceptor**
Nociceptors are known as small-diameter DRG neurons with unmyelinated C-fibers or thinly myelinated Aδ fibers that convey peripheral nociceptive signals to laminae I and II of the spinal cord. The present study showed that *Zcchc12*^{+} DRG neurons could be a specific type of peptidergic nociceptors. The peptidergic neurons release a variety of neuropeptides to modulate the pain transmission (Basbaum et al., 2009). Genetically, *Zcchc12*^{+} DRG neurons could express *Calca*, *Gal*, tachykinin 1 (*Tac1*), and

adenylate cyclase activating polypeptide 1 (*Adcyap1*). They are all well-known modulators for nociceptive perception (Lang et al., 2007; Lang and Kofler, 2011). The *Gal*-KO mice showed abnormal nociceptive responsiveness (Kerr et al., 2000). Lack of *Tac1* prevents nociceptors from properly encoding the nociceptive stimulus in mice (Gutierrez et al., 2019). Moreover, *Zcchc12*^{+} neurons also expressed important functional channels for nociceptors, such as the *Scn9a*, *Scn10a*, *Scn11a*, and *Trpv1* (Dib-Hajj et al., 2010). The gene profile in *Zcchc12*^{+} DRG neurons implies that they could function as peptidergic nociceptors.

Zcchc12^{+} neurons were the smallest DRG neurons, and centrally projected to lamina I-II$_{\text{outer}}$ of the spinal dorsal horn, which was inconsistent with the projection pattern of CGRP[+] peptidergic C fibers transmitting nociceptive signals. Peripherally, *Zcchc12*^{+} neurons innervated the glabrous skin by free nerve endings, which provided the structural basis for noxious heat sensation (Zylka et al., 2005). We also observed the clustered nerve terminals of *Zcchc12*^{+} DRG neurons surrounding the footpads. Morphologically, the *Zcchc12*^{+} cluster of endings in the footpad might innervate sweat glands, which may imply a possible function of the *Zcchc12*^{+} DRG neurons in interaction with sympathetic neurons for regulating the functions of sweat glands. Since humans did not have the footpads, the specialized clustered nerve terminals were not reported in human tissue. In addition, the *Zcchc12*^{+} circumferential endings were observed in hairy skin. Since *Zcchc12*^{+} DRG neurons could function as peptidergic nociceptors, the specific circumferential endings might mediate mechanical pain as *Calca*[+] circumferential endings as reported by Ghitani et al. (2017). This evidence provides the distribution pattern of *Zcchc12*^{+} fibers in the skin and spinal dorsal horn, a basis that *Zcchc12*^{+} DRG neurons might be involved in the sensation of heat and mechanical pain.

Zcchc12[+] DRG neuron is essential for noxious heat sensation

A large portion of DRG neurons function as polymodal mechanoheat nociceptors with different sensitivity to peripheral stimulations. For example, *Sst*[+], *Mrgpra3*^{+}, and *Mrgprd*^{+} DRG neurons present higher sensitivity to pruritic stimuli. *Mrgprd*^{+} DRG neurons also play a vital role in mediating mechanical pain. In this study, we identified that *Zcchc12*^{+} DRG neurons displayed the feature of polymodal nociceptors and were more sensitive to noxious heat than to mechanical stimuli. The molecular basis of this feature could be attributed to thermal-related genes highly expressed in *Zcchc12*^{+} DRG neurons. The TRP genes, which play essential roles in thermal sensation, including TRPV1, TRPA1, TRPM3, and TRPV2, were detected to be expressed in *Zcchc12*^{+} DRG neurons (C. L. Li et al., 2016; K. Wang et al., 2021). TRPV1-deficient mice showed impaired behavioral responses to noxious thermal stimuli (Caterina et al., 1997, 2000). TRPV2 was activated by high temperatures (>52°C) and contributed to heat-evoked nociception (Lewinter et al., 2004; Yao et al., 2011). However, TRPV2 gene deficiency has no significant effect on thermal nociception (Park et al., 2011). TRPM3 could be activated by heating, and lack of TRPM3 hampered the nociceptive responses to noxious heat (Vriens et al., 2011). TRPA1 was only expressed in a subset of *Zcchc12*^{+} DRG neurons. Thus, TRPA1 might not be the main component in our present study. We considered that selective ablation of *Zcchc12*^{+} DRG neurons might abolish the functions of *Trpv1*, *Trpm3*, and other genes in mice, which led to mouse insensitive to noxious heat.

Zcchc12^{+} DRG neurons could also express the mechanosensors, including KCNKs, ASICs, and TACAN, a newly identified ion channel involving sensation of mechanical pain (Beaulieu-Laroche et al., 2020). However, selective ablation of *Zcchc12*^{+} DRG neurons did not impair the mechanical sensation under physiological or pathologic conditions, implying that the mechanosensors were also contained in other types of DRG neurons. A previous report showed that ablation of *Mrgprd*^{+} neurons in the DRG caused the defect of mechanosensation but not thermal sensation (Cavanaugh et al., 2009), although *Mrgprd*^{+} DRG neurons could respond to noxious heat and mechanical stimuli in *ex vivo* electrophysiological recording (Rau et al., 2009). Additionally, a relatively high level of *Trpm8*, a gene encoding a cold-sensing molecule, was specifically expressed by a subtype of *Zcchc12*^{+} neurons in the DRG (K. Wang et al., 2021). Nevertheless, selective ablation of *Zcchc12*^{+} neurons was not able to affect the cold sensation in mice, suggesting that *Zcchc12*^{+} DRG neurons were not essential for cold sensation. There might be other DRG neurons that express *TRPM8* at a low level, or other molecules may be involved in cold sensation. Therefore, the ability of *Zcchc12*^{+} DRG neurons responsive to mechanical and cold stimuli may serve as a substitutive effect.

In vivo calcium imaging in the DRG showed that *Zcchc12*^{+} neurons could be activated not only by noxious heat, but also by mechanical stimuli and noxious cold. According to our 10× Genomics scRNA-seq data, *Zcchc12*^{+} DRG neurons could further be divided into four subtypes, including *Zcchc12*^{+}/*Sstr2*^{+}, *Zcchc12*^{+}/*Dcn2*^{+}, *Zcchc12*^{+}/*Trpm8*^{+}, and *Zcchc12*^{+}/*Rxfp1*^{+} neurons (K. Wang et al., 2021). About half of *Zcchc12*^{+} DRG neurons express CGRP. *Zcchc12*^{+}/*Trpm8*^{+} DRG neurons express substance P, a neuropeptide encoded by *Tac1*, but not CGRP (K. Wang et al., 2021), which is in accordance with the data reported by Ginty's laboratory (Sharma et al., 2020). The heterogeneity of *Zcchc12*^{+} DRG neurons indicated their functional variety, which requires further investigation. Trpm8 was only contained in a part of *Zcchc12*^{+} neurons, which could be the reason that only 16% of recorded *Zcchc12*^{+} neurons responded to noxious cold.

References

Abraira VE, Ginty DD (2013) The sensory neurons of touch. Neuron 79:618–639.

Akopian AN, Souslova V, England S, Okuse K, Ogata N, Ure J, Smith A, Kerr BJ, McMahon SB, Boyce S, Hill R, Stanfa LC, Dickenson AH, Wood JN (1999) The tetrodotoxin-resistant sodium channel SNS has a specialized function in pain pathways. Nat Neurosci 2:541–548.

Bai L, Lehnert BP, Liu J, Neubarth NL, Dickendesher TL, Nwe PH, Cassidy C, Woodbury CJ, Ginty DD (2015) Genetic identification of an expansive mechanoreceptor sensitive to skin stroking. Cell 163:1783–1795.

Basbaum AI, Bautista DM, Scherrer G, Julius D (2009) Cellular and molecular mechanisms of pain. Cell 139:267–284.

Beaulieu-Laroche L, et al. (2020) TACAN is an ion channel involved in sensing mechanical pain. Cell 180:956–967.e917.

Caterina MJ, Schumacher MA, Tominaga M, Rosen TA, Levine JD, Julius D (1997) The capsaicin receptor: a heat-activated ion channel in the pain pathway. Nature 389:816–824.

Caterina MJ, Leffler A, Malmberg AB, Martin WJ, Trafton J, Petersen-Zeitz KR, Koltzenburg M, Basbaum AI, Julius D (2000) Impaired nociception and pain sensation in mice lacking the capsaicin receptor. Science 288:306–313.

Cavanaugh DJ, Lee H, Lo L, Shields SD, Zylka MJ, Basbaum AI, Anderson DJ (2009) Distinct subsets of unmyelinated primary sensory fibers mediate behavioral responses to noxious thermal and mechanical stimuli. Proc Natl Acad Sci USA 106:9075–9080.

Cho G, Lim Y, Zand D, Golden JA (2008) Sizn1 is a novel protein that functions as a transcriptional coactivator of bone morphogenic protein signaling. Mol Cell Biol 28:1565–1572.

Cho G, Lim Y, Golden JA (2011) XLMR candidate mouse gene, *Zcchc12* (Sizn1) is a novel marker of Cajal-Retzius cells. Gene Expr Patterns 11:216–220.

Dhaka A, Viswanath V, Patapoutian A (2006) Trp ion channels and temperature sensation. Annu Rev Neurosci 29:135–161.

Dib-Hajj SD, Cummins TR, Black JA, Waxman SG (2010) Sodium channels in normal and pathological pain. Annu Rev Neurosci 33:325–347.

Garrison SR, Dietrich A, Stucky CL (2012) TRPC1 contributes to light-touch sensation and mechanical responses in low-threshold cutaneous sensory neurons. J Neurophysiol 107:913–922.

Ghitani N, Barik A, Szczot M, Thompson JH, Li C, Le Pichon CE, Krashes MJ, Chesler AT (2017) Specialized mechanosensory nociceptors mediating rapid responses to hair pull. Neuron 95:944–954.

Gutierrez S, Alvarado-Vazquez PA, Eisenach JC, Romero-Sandoval EA, Boada MD (2019) Tachykinins modulate nociceptive responsiveness and sensitization: in vivo electrical characterization of primary sensory neurons in tachykinin knockout (Tac1 KO) mice. Mol Pain 15:1744806919845750.

Han L, Dong X (2014) Itch mechanisms and circuits. Annu Rev Biophys 43:331–355.

Han L, Ma C, Liu Q, Weng HJ, Cui Y, Tang Z, Kim Y, Nie H, Qu L, Patel KN, Li Z, McNeil B, He S, Guan Y, Xiao B, Lamotte RH, Dong X (2013) A subpopulation of nociceptors specifically linked to itch. Nat Neurosci 16:174–182.

Julius D (2013) TRP channels and pain. Annu Rev Cell Dev Biol 29:355–384.

Kandel ER, Schwartz JH, Jessell TM, Siegelbaum SA, Hudspeth AJ (2013) Principles of neural science [M], Ed 5. New York: McGraw-Hill.

Kerr BJ, Cafferty WB, Gupta YK, Bacon A, Wynick D, McMahon SB, Thompson SW (2000) Galanin knockout mice reveal nociceptive deficits following peripheral nerve injury. Eur J Neurosci 12:793–802.

Lang R, Kofler B (2011) The galanin peptide family in inflammation. Neuropeptides 45:1–8.

Lang R, Gundlach AL, Kofler B (2007) The galanin peptide family: receptor pharmacology, pleiotropic biological actions, and implications in health and disease. Pharmacol Ther 115:177–207.

Lewinter RD, Skinner K, Julius D, Basbaum AI (2004) Immunoreactive TRPV-2 (VRL-1), a capsaicin receptor homolog, in the spinal cord of the rat. J Comp Neurol 470:400–408.

Li CL, Li KC, Wu D, Chen Y, Luo H, Zhao JR, Wang SS, Sun MM, Lu YJ, Zhong YQ, Hu XY, Hou R, Zhou BB, Bao L, Xiao HS, Zhang X (2016) Somatosensory neuron types identified by high-coverage single-cell RNA-sequencing and functional heterogeneity. Cell Res 26:83–102.

Li L, Rutlin M, Abraira VE, Cassidy C, Kus L, Gong S, Jankowski MP, Luo W, Heintz N, Koerber HR, Woodbury CJ, Ginty DD (2011) The functional organization of cutaneous low-threshold mechanosensory neurons. Cell 147:1615–1627.

Li QL, Chen FJ, Lai R, Guo ZM, Luo R, Yang AK (2012) ZCCHC12, a potential molecular marker of papillary thyroid carcinoma: a preliminary study. Med Oncol 29:1409–1417.

Li WG, Xu TL (2011) ASIC3 channels in multimodal sensory perception. ACS Chem Neurosci 2:26–37.

McCoy ES, Taylor-Blake B, Zylka MJ (2012) CGRPalpha-expressing sensory neurons respond to stimuli that evoke sensations of pain and itch. PLoS One 7:e36355.

McCoy ES, Taylor-Blake B, Street SE, Pribisko AL, Zheng J, Zylka MJ (2013) Peptidergic CGRPalpha primary sensory neurons encode heat and itch and tonically suppress sensitivity to cold. Neuron 78:138–151.

Meixiong J, Dong X (2017) Mas-related G protein-coupled receptors and the biology of itch sensation. Annu Rev Genet 51:103–121.

Meyer RA, Ringkamp M, Campbell JN, Raja SN (2006) Wall and Melzack's textbook of pain, Ed 5. London: Elsevier.

Nassar MA, Stirling LC, Forlani G, Baker MD, Matthews EA, Dickenson AH, Wood JN (2004) Nociceptor-specific gene deletion reveals a major role for Nav1.7 (PN1) in acute and inflammatory pain. Proc Natl Acad Sci USA 101:12706–12711.

Noel J, Zimmermann K, Busserolles J, Deval E, Alloui A, Diochot S, Guy N, Borsotto M, Reeh P, Eschalier A, Lazdunski M (2009) The mechano-activated K⁺ channels TRAAK and TREK-1 control both warm and cold perception. EMBO J 28:1308–1318.

Park U, Vastani N, Guan Y, Raja SN, Koltzenburg M, Caterina MJ (2011) TRP vanilloid 2 knock-out mice are susceptible to perinatal lethality but display normal thermal and mechanical nociception. J Neurosci 31:11425–11436.

Rau KK, McIlwrath SL, Wang H, Lawson JJ, Jankowski MP, Zylka MJ, Anderson DJ, Koerber HR (2009) Mrgprd enhances excitability in specific populations of cutaneous murine polymodal nociceptors. J Neurosci 29:8612–8619.

Sharma N, Flaherty K, Lezgiyeva K, Wagner DE, Klein AM, Ginty DD (2020) The emergence of transcriptional identity in somatosensory neurons. Nature 577:392–398.

Stantcheva KK, Iovino L, Dhandapani R, Martinez C, Castaldi L, Nocchi L, Perlas E, Portulano C, Pesaresi M, Shirlekar KS, de Castro Reis F, Paparountas T, Bilbao D, Heppenstall PA (2016) A subpopulation of itch-sensing neurons marked by Ret and somatostatin expression. EMBO Rep 17:585–600.

Stuart T, Satija R (2019) Integrative single-cell analysis. Nat Rev Genet 20:257–272.

Usoskin D, Furlan A, Islam S, Abdo H, Lonnerberg P, Lou D, Hjerling-Leffler J, Haeggstrom J, Kharchenko O, Kharchenko PV, Linnarsson S, Ernfors P (2015) Unbiased classification of sensory neuron types by large-scale single-cell RNA sequencing. Nat Neurosci 18:145–153.

Vriens J, Owsianik G, Hofmann T, Philipp SE, Stab J, Chen X, Benoit M, Xue F, Janssens A, Kerselaers S, Oberwinkler J, Vennekens R, Gudermann T, Nilius B, Voets T (2011) TRPM3 is a nociceptor channel involved in the detection of noxious heat. Neuron 70:482–494.

Wang K, Wang S, Chen Y, Wu D, Hu X, Lu Y, Wang L, Bao L, Li C, Zhang X (2021) Single-cell transcriptomic analysis of somatosensory neurons uncovers temporal development of neuropathic pain. Cell Res 31:904–918.

Wang O, Zheng Z, Wang Q, Jin Y, Jin W, Wang Y, Chen E, Zhang X (2017) ZCCHC12, a novel oncogene in papillary thyroid cancer. J Cancer Res Clin Oncol 143:1679–1686.

Woo SH, Lukacs V, de Nooij JC, Zaytseva D, Criddle CR, Francisco A, Jessell TM, Wilkinson KA, Patapoutian A (2015) Piezo2 is the principal mechanotransduction channel for proprioception. Nat Neurosci 18:1756–1762.

Yang L, Dong F, Yang Q, Yang PF, Wu R, Wu QF, Wu D, Li CL, Zhong YQ, Lu YJ, Cheng X, Xu FQ, Chen L, Bao L, Zhang X (2017) FGF13 selectively regulates heat nociception by interacting with Nav1.7. Neuron 93:806–821.e809.

Yao J, Liu B, Qin F (2011) Modular thermal sensors in temperature-gated transient receptor potential (TRP) channels. Proc Natl Acad Sci USA 108:11109–11114.

Zheng Y, Liu P, Bai L, Trimmer JS, Bean BP, Ginty DD (2019) Deep sequencing of somatosensory neurons reveals molecular determinants of intrinsic physiological properties. Neuron 103:598–616.

Zylka MJ, Rice FL, Anderson DJ (2005) Topographically distinct epidermal nociceptive circuits revealed by axonal tracers targeted to Mrgprd. Neuron 45:17–25.